Electronic Supplementary Material (ESI) for Lab on a Chip.

Supporting Information - Arends et al.

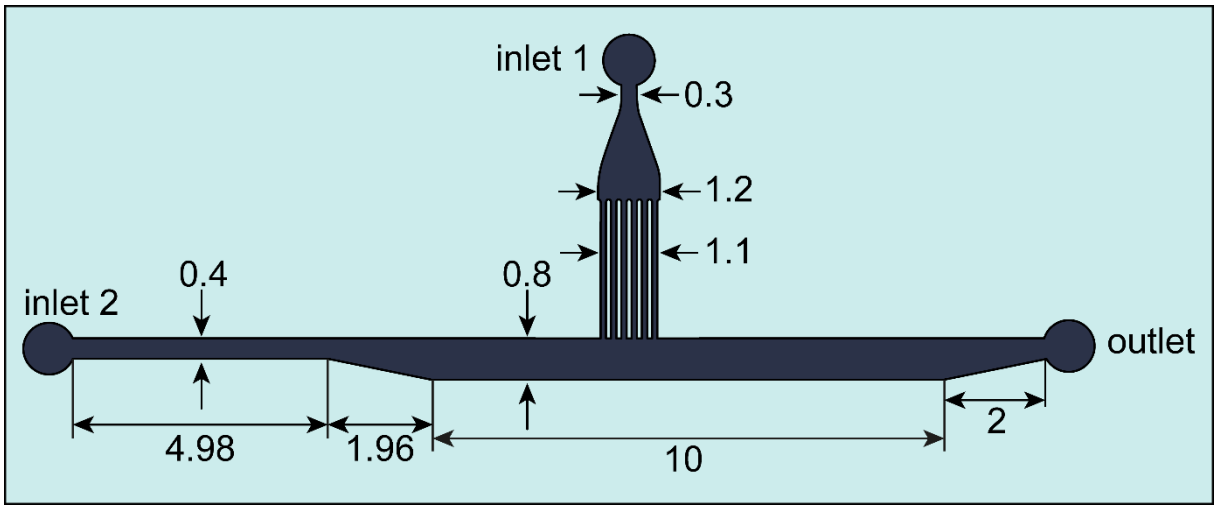

Figure S1. Detailed scheme of the microfluidic setup; all dimensions are given in mm.

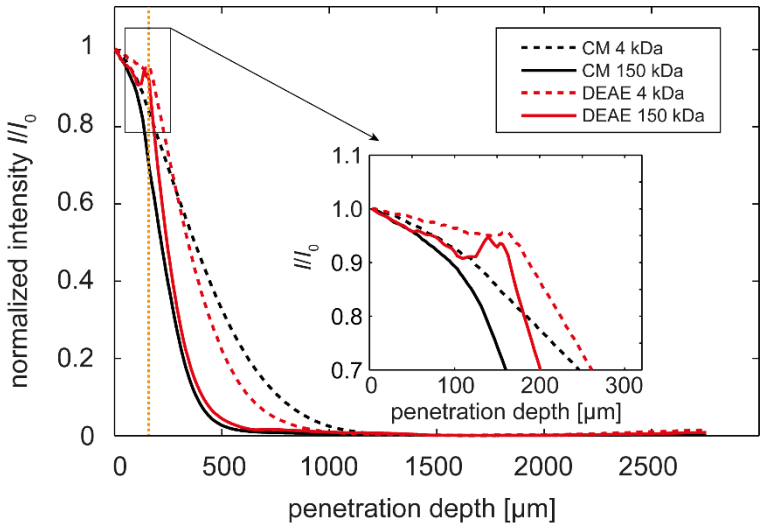

Figure S2. Intensity profiles for dextrans as acquired 5 min after insertion into the microfluidics channel. The 4 kDa dextrans (dashed lines) penetrate more deeply into the channel than the 150 kDa variants. We observe a small accumulation peak at the ECM/buffer interface (marked by the orange dotted line) for both positively charged DEAE-dextrans (red dashed line: 4 kDa; red line: 150 kDa), whereas no accumulation is observed for the negatively charged CM-dextrans.

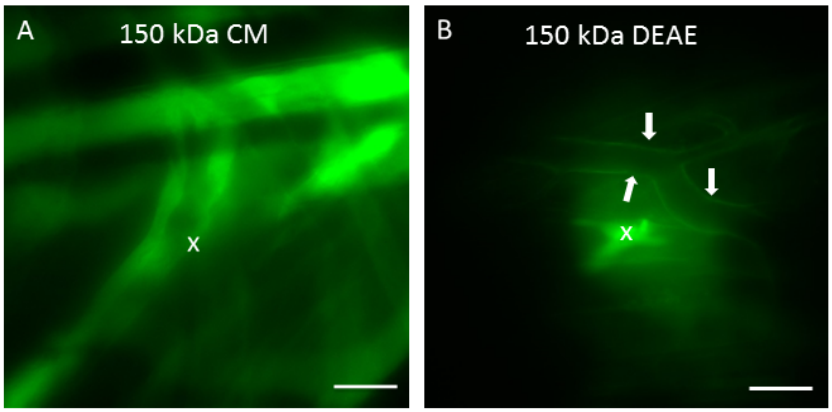

Figure S3. Fluorescence images showing the distribution of negatively charged CM (A) and positively charged DEAE (B) dextrans (MW = 150 kDa) 5 min after microinjection into the cremaster muscle of a mouse. The CM-dextrans rapidly spread from the injection site (white cross) next to muscle fibers (A) whereas the DEAE-dextrans accumulate around blood vessels (white arrows, B). Scale bar: 50 µm.

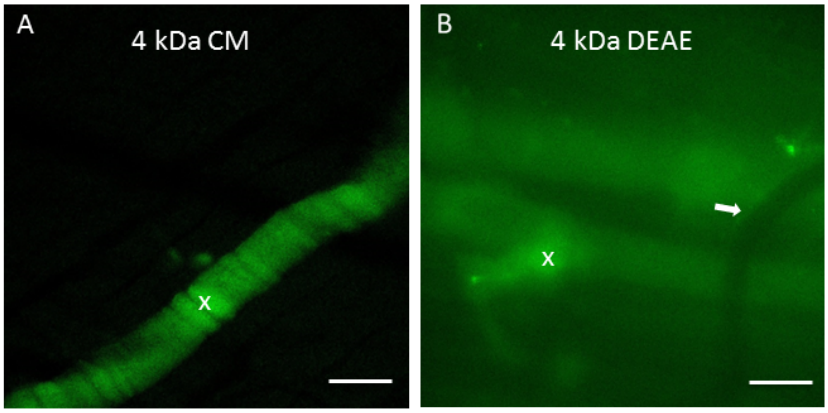

Figure S4. Fluorescence images showing the distribution of negatively charged CM (A) and positively charged DEAE (B) dextrans (MW = 4 kDa) 60 min after microinjection into the murine cremaster muscle. The CM-dextrans accumulate at the injection site (white cross) along muscle fibers (A) whereas the DEAE-dextrans remain in the interstitial space and around blood vessels (white arrows, B). Scale bar: 50 µm.

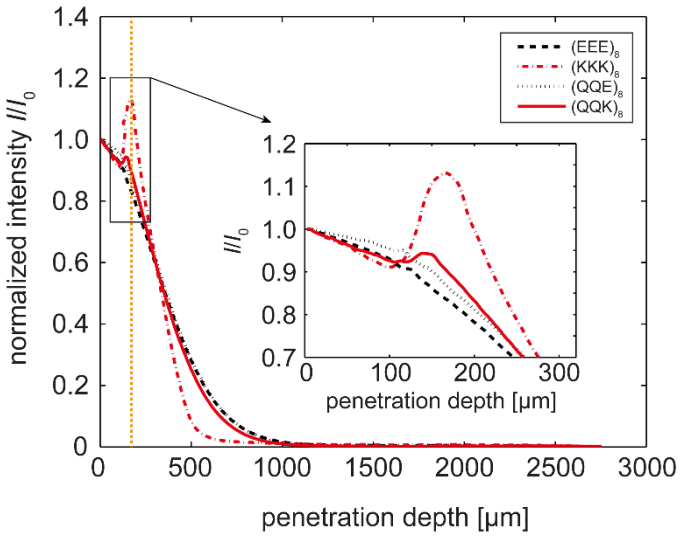

Figure S5. Intensity profiles for peptides as acquired 5 min after insertion into the microfluidics channel. Beyond the buffer/gel interface, the penetration profiles are similar for all peptide variants. For the $(QQK)_8$ peptides, we observe a small accumulation peak at the ECM/buffer interface (marked by the orange dotted line). We measure an accumulation peak intensity of 94 % of the channel intensity. For the higher positively charged $(KKK)_8$ peptides, the accumulation is stronger with a peak intensity of 113 %. Negatively charged $(EEE)_8$ and $(QQE)_8$ peptides show no accumulation at the interface.

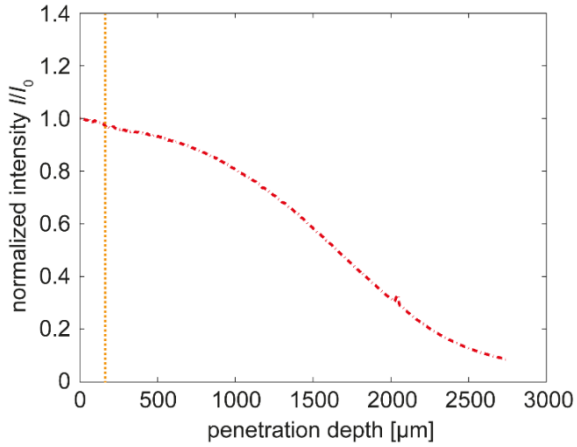

Figure S6. Intensity profile of $(KKK)_8$ penetration into a bovine collagen I gel 25 min after insertion. The collagen I was prepared as suggested by the manufacturer (Life Technologies, Darmstadt, Germany), and the gel was prepared at a final concentration of 3 mg/mL. In contrast to the experiments with ECM, no accumulation of the positively charged peptide is observed at the collagen/buffer interface which is marked by the orange dotted line.

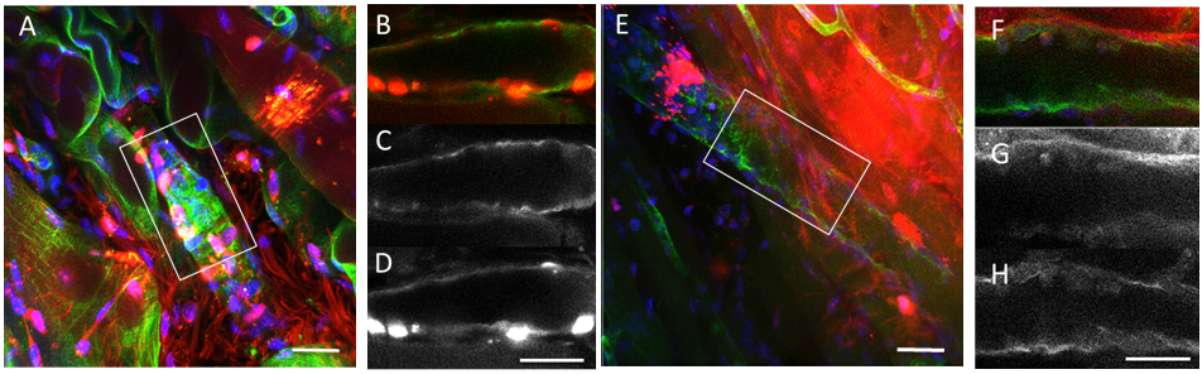

Figure S7. Confocal immunofluorescence images of $(KKK)_8$ peptides 60 min after microinjection into the murine cremaster muscle. (A) and (E) show 3D rendered images of 20 confocal z-planes (1 µm distance) of postcapillary venules in the muscle tissue. Single confocal z-planes from the regions indicated in (A) and (E) are shown in (B-D) and (F-H). Cell nuclei are depicted in blue (TO-PRO3), Collagen IV green (A, B and D) and CD31, which marks endothelial cells green in (E, F and H). The $(KKK)_8$ peptide (red A, B, D, E, F and G) co-localizes with collagen IV at the basolateral side of endothelial cells. Scale bar: 30 µm.

Simulation of molecule diffusion and binding to the gel

As a general description of the diffusive process we used a standard reaction-diffusion model in one dimension that includes the binding and unbinding processes to the gel. We set up a system of two coupled partial differential equations for the time dependent evolution of the corresponding concentrations of the bound and the unbound part:

$$\frac{\partial c_u}{\partial t} = D\frac{\partial^2 c_u}{\partial x^2} + R$$
$$\frac{\partial c_b}{\partial t} = -R$$

Here, c_u and c_b denote the unbound and the bound concentration, respectively, and D is the diffusion coefficient. The reaction part $\pm R$ of the equations describes the binding to and the unbinding from the gel.

In the simulation, we assumed that a reservoir of infinite size with concentration $c_u = 1$ is coupled to a small intermediate buffer region at position $x = 0$. The gel extends from $x = 0.05$ to the right boundary at $x = L$, where we applied absorbing boundary conditions (i.e. an infinitely large reservoir of concentration $c_u = c_b = 0$). Since binding and unbinding rates are directly proportional to the corresponding concentrations we obtain linear reactions terms:

$$R = k^{off} c_b - k^{on} c_u$$

The rate constants for binding and unbinding are given by k^{on} and k^{off}, respectively. To take into account that both, binding and unbinding processes can only take place in the gel (i.e. in the region $0.05 < x < 1$), the rate constants have to be chosen such that:

$$k^{on} = k^{off} = 0 \text{ for } x < 0.05$$

By inserting the reaction part into the reaction-diffusion we obtain:

$$\frac{\partial c_u}{\partial t} = D \frac{\partial^2 c_u}{\partial x^2} + k^{off} c_b - k^{on} c_u \tag{1}$$

$$\frac{\partial c_b}{\partial t} = -k^{off} c_b + k^{on} c_u \tag{2}$$

These partial differential equations describe the full time evolution of the reaction-diffusion system in the gel. The total concentration is given by the sum of the bound and the unbound part:

$$c_{tot}(x,t) = c_u(x,t) + c_b(x,t)$$

For a numerical simulation of the reaction-diffusion model, the equations (1) and (2) have to be discretized in space and time. Therefore, a grid of N_x equally spaced points with distance $\Delta x = l / N_x$ is introduced. From considerations of numerical stability a fixed time step is

chosen. The solution is propagated stepwise in time by an Euler-Forward scheme. The discretized equations read:

$$c_{u,j}^{k+1} = c_{u,j}^{k} + \Delta t\left(\frac{D}{\Delta x^2}\left[c_{u,j+1}^{k} - 2c_{u,\mathrm{j}}^{k} + c_{u,j-1}^{k}\right] + k^{off}c_{b,j}^{k} - k^{on}c_{u,j}^{k}\right)$$

$$c_{b,j}^{k+1} = c_{b,j}^{k} + \Delta t\left(-k^{off}c_{b,j}^{k} + k^{on}c_{u,j}^{k}\right)$$

where $x = j\Delta x$ and $t = k\Delta t$. This was implemented in Matlab and calculated for the parameters shown in Table S1.

The model allows for a continuous fast diffusion of molecules to the interface. However, when the molecules reach the interface, the binding affinity of the molecules to the gel results in a "slowed down" diffusion from the interface back into the buffer compartment due to binding events. This results in an effective asymmetric diffusion and gives rise to the concentration peak at the interface.

Table S1: Parameter choice for the calculation of penetration profiles.

Parameter	Value	Description
D	$2*10^{-5}$	Diffusion coefficient
k^{on}	(1) $2*10^{-4}$ (2) $2*10^{-5}$	on rate (red dash-dotted line in Fig. 3 of the main paper) on rate (red line in Fig. 3 of the main paper)
k^{off}	(1) $2*10^{-5}$ (2) $2*10^{-6}$	off rate (red dash-dotted line in Fig. 3 of the main paper) off rate (red line in Fig. 3 of the main paper)